Canterbury
Christ Church
University

Research Space
Journal article

Fermentation of biomass-generated synthesis gas: effects of nitric oxide

Ahmed, A. and Lewis, R.S.

Fermentation of Biomass-Generated Synthesis Gas: Effects of Nitric Oxide

Asma Ahmed,[1] Randy S. Lewis[2]

[1]Biosystems and Agricultural Engineering, Oklahoma State University, Stillwater, Oklahoma
[2]Chemical Engineering Department, 350 CB, Brigham Young University, Provo, Utah 84602;
Email: randy.lewis@byu.edu

ABSTRACT:

The production of renewable fuels, such as ethanol, has been steadily increasing owing to the need for a reduced dependency on fossil fuels. It was demon-strated previously that biomass-generated synthesis gas (biomass-syngas) can be converted to ethanol and acetic acid using a microbial catalyst. The biomass-syngas (pri-marily CO, CO_2, H_2, and N_2) was generated in a fluidized-bed gasifier and used as a substrate for *Clostridium carboxidivorans* P7^T. Results showed that the cells stopped consuming H_2 when exposed to biomass-syngas, thus indicating that there was an inhibition of the hydrogenase enzyme due to some biomass-syngas contaminant. It was hypothesized that nitric oxide (NO) detected in the bio-mass-syngas could be the possible cause of this inhibition. The specific activity of hydrogenase was monitored with time under varying concentrations of H_2 and NO. Results indicated that NO (at gas concentrations above 40 ppm) was a non-competitive inhibitor of hydrogenase activity, although the loss of hydrogenase activity was reversible. In addition, NO also affected the cell growth and increased the amount of ethanol produced. A kinetic model of hydro-genase activity with inhibition by NO was demonstrated with results suggesting there are multiple binding sites of NO on the hydrogenase enzyme. Since other syngas-fermenting organisms utilize the same metabolic pathways, this study estimates that NO < 40 ppm can be tolerated by cells in a syngas-fermentation system without compromising the hydrogenase activity, cell growth, and product distribution.

KEYWORDS: syngas; ethanol; fermentation; biomass; hydrogenase

Introduction

The production of renewable fuels such as ethanol has been steadily increasing, owing to the need for a reduced dependency on fossil fuels. Ethanol is currently used as an additive to gasoline to enhance the fuel efficiency, as well as to reduce toxic emissions such as CO, CO_2, NO_x, and hydrocarbons (He et al., 2003; Hsieh et al., 2002; Yuksel and Yuksel, 2004). Ethanol is a promising alternative fuel due to its biodegradability and regenerative characteristics and is being projected as a substitute for MTBE, as it would reduce water contamination and the adverse effects on public health (He et al., 2003; Nadim et al., 2001).

Research has been extensive on the various processes used for ethanol production from biomass. One process involves the gasification of biomass, such as Switchgrass, to produce a gas mixture primarily containing CO, CO_2, H_2, and N_2. The biomass-generated synthesis gas (biomass-syngas) is then fermented by microbial catalysts to form alcohols and acids. Anaerobic bacteria, such as *Clostridium ljungdahlii* and *Clostridium autoethanogenum*, have been shown to convert CO, CO_2, and H_2 to ethanol and acetic acid (Abrini et al., 1994; Vega et al., 1990).

Many of the reported fermentation efforts have involved the utilization of simulated or "synthetic" syngas prepared from mixtures of purchased gases. Unlike synthetic syngas, biomass-syngas often contains additional constitu-ents including methane, some higher hydrocarbons, tars, ash, and char particles as a result of the gasification process (Bridgwater, 1994). However, there has been very little work published on the effects of biomass-syngas impurities on fermentation processes (Spath and Dayton, 2003). An understanding of the potential contaminants on the fermentation process is essential for assessing the degree to which biomass-syngas must be cleaned. Recent work (Datar

et al., 2004) showed the integration of a fluidized-bed gasifier with a bioreactor to utilize biomass-syngas to produce ethanol. A novel anaerobic bacterium, *Clostridium carboxidivorans* P7[T] (Liou et al., 2005) was used as the microbial catalyst. Certain effects of the biomass-syngas were observed on the fermentation process, including cell dormancy (cell growth was dormant but product formation was active), shutdown of H_2 consumption, and product redistribution between ethanol and acetic acid (Datar et al., 2004). Our recent studies have shown that cell dormancy can be overcome with a 0.025 μm filter, but not the traditional sterilization filter size of 0.2 μm (Ahmed et al., 2006). Filter analysis showed the capture of small particulates that appeared to be tars. Further analysis demonstrated that tars indeed prolonged cell growth. However, use of the 0.025 μm filter did not prevent the shutdown of H_2 consumption by the cells. The hypothesis was that a gaseous species permeating through the filter was responsible for the shutdown of H_2 consumption.

Gases such as O_2 (Seefeldt and Arp, 1989), acetylene, CO, and nitric oxide (NO) are known inhibitors of hydrogenase (Acosta et al., 2003; Kim et al., 1984; Krasna and Rittenberg, 1954; Tibelius and Knowles, 1984). Studies have shown NO to inhibit hydrogenase activity in *Azotobacter vinelandii* (Hyman and Arp, 1991), *Proteus vulgaris* (Krasna and Rittenberg, 1954), *Alcaligenes eutrophus* (Hyman and Arp, 1988), and *Azospirillum brasilense* (Tibelius and Knowles, 1984) although a quantitative analysis of the effects of NO on clostridial hydrogenase has not been performed. For the previous work using biomass-syngas in which H_2 consumption was shut down, approximately 140–150 ppm of NO was detected in the biomass-generated syngas using a chemiluminescence analyzer. Though gasification processes typically contain ammonia rather than NO (Devi et al., 2003), the presence of NO in the syngas could be due to some pockets of combustion within the gasifier.

C. carboxidivorans P7[T] and other syngas-fermenting organisms use the Acetyl-CoA pathway to convert CO, CO_2, and H_2 into biomass, ethanol, acetic acid, and other products. Figure 1 shows the acetyl-CoA pathway in which CO and CO_2 are converted to acetyl-CoA (Ragsdale, 1991). The electrons required for this conversion are obtained from H_2, via the hydrogenase enzyme, or from CO, via the carbon monoxide dehydrogenase (CODH) enzyme. If the hydrogenase enzyme is inhibited, the cells cannot consume H_2 and the electrons must come from CO. This scenario is inefficient for ethanol production since the CO is sacrificed for electrons rather than used for product formation. Therefore, it is important to assess the cause and extent of hydrogenase inhibition in order to design a fermentation process that can utilize H_2 from biomass-syngas. This work describes the effects of NO on the hydrogenase activity, cell growth, and product distribution of *C. carboxidivorans* P7[T]. This study also indicates the levels of NO that can be tolerated by cells without compromising the hydrogenase activity.
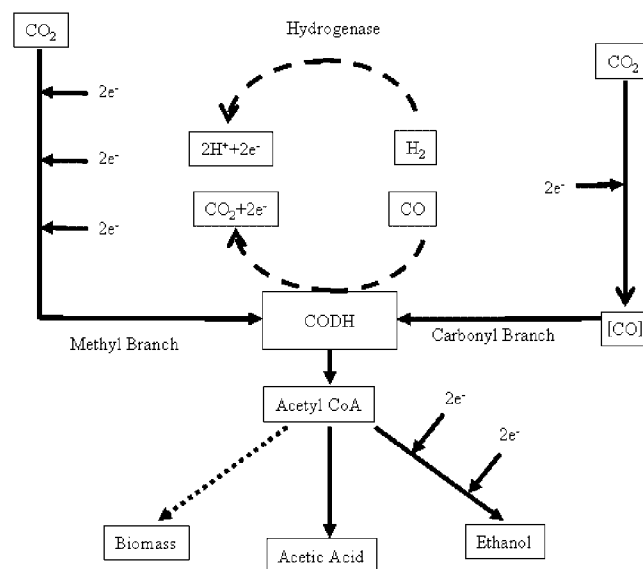

Figure 1. Schematic of the acetyl-CoA pathway showing the utilization of CO, CO_2, and H_2 to ethanol, acetic acid, and biomass. The hydrogenase enzyme is utilized to produce electrons. CODH, carbon monoxide dehydrogenase enzyme.

Materials and Methods

Microbial Catalyst and Culture Medium

C. carboxidivorans P7[T], provided by Dr. Ralph Tanner, University of Oklahoma, was utilized for the fermentation. The bacterium was grown under strictly anaerobic conditions in a medium containing (per liter) 30 mL mineral stock solution, 10 mL trace metal stock solution, 10 mL vitamin stock solution, 0.5 g yeast extract, 5 g morpholinoethanesulfonic acid (MES), and 10 mL of 4% cysteine-sulfide solution. Resazurin solution (0.1%) was added as a redox indicator. The mineral stock solution contained (per liter) 80 g sodium chloride, 100 g ammonium chloride, 10 g potassium chloride, 10 g potassium monophosphate, 20 g magnesium sulfate, and 4 g calcium chloride. The vitamin stock solution contained (per liter) 0.01 g pyridoxine, 0.005 g thiamine, 0.005 g riboflavin, 0.005 g calcium pantothenate, 0.005 g thioctic acid, 0.005 g amino benzoic acid, 0.005 g nicotinic acid, 0.005 g vitamin B12, 0.002 g biotin, 0.002 g folic acid, and 0.01 g 2-mercaptoethanesulfonic acid sodium salt (MESNA). The stock solution of trace metals contained (per liter) 2 g nitrilotriacetic acid, 1 g manganese sulfate, 0.8 g ferrous ammonium sulfate, 0.2 g cobalt chloride, 0.2 g zinc sulfate, 0.02 g copper chloride, 0.02 g nickel chloride, 0.02 g sodium molybdate, 0.02 g sodium selenate, and 0.02 g sodium tungstate.

Experimental Method

Two 500 mL Cytostir[®] cell culture flasks (Kontes/Kimble Glass, Inc., Vineland, NJ) were used for the experiments.

Each sampling arm contained a rubber stopper for inoculation, sampling, and gas sparging. One liter of media, excluding the cysteine-sulfide, was prepared and equally distributed into both flasks, following which the flasks were autoclaved at 121°C for 20 min. After cooling, the media was continuously purged with N_2 to provide an anaerobic environment. The flasks were then placed in a water bath at 37°C. The water bath was placed on magnetic stir plates to provide agitation. The water-bath level was always maintained such that the liquid level in the flasks was below that of the water bath. Cysteine-sulfide (5 mL) was added to each flask to scavenge any remaining dissolved oxygen.

Following the presence of an anaerobic environment, continuous gas sparging of the feed gases at 10 mL/min was initiated via the use of 18G luer needles for the inlet and outlet. Flask A was initially sparged with a gas mixture containing 20% CO, 15% CO_2, 5% H_2, and balance N_2 (Air Liquide, Houston, TX). Flask B was initially sparged with 20% CO and 15% CO_2, with the concentrations of NO and H_2 ranging between 0–160 ppm and 2.5–15%, respectively. Combinations of gas cylinders containing CO, CO_2, H_2, N_2, and NO were mixed using mass flow controllers to obtain the appropriate concentrations. With gas flow initiated, 5mL of inoculum was added to each flask.

Samples (1.5 mL) were taken periodically from each flask to measure the optical density (OD), pH, and product concentrations. Samples for hydrogenase activity (0.4–0.6 mL) and gas compositions (20 μL) were also obtained. In experiments with more than 40 ppm of NO in the gas stream, it was seen that the cells could not grow in the presence of NO (Flask B) at the beginning of the run. In these experiments, the gas sources were switched between Flask A and Flask B once the cells in Flask A had reached a constant concentration. The gases were switched to determine the effects of NO on active cells and also to determine whether the inhibition of growth by NO was reversible. In some experiments, the gases were switched back again to their original compositions to once again determine the reversibility of the effects of NO on growth and hydrogenase activity.

Hydrogenase Assay

For the hydrogenase assay, benzyl viologen was used as the electron acceptor and a nonionic detergent, triton X-100 was used to permeabilize the cell membranes. The assay buffer contained 0.4 mL 1 M Tris-HCl, 0.2 mL 0.04 M benzyl viologen, 0.1 mL 5% v/v Triton X-100, 0.2 mL 0.04 M dithiothreitol, and 3 mL degassed DI water (Shenkman, 2003). All the above reagents, except for dithiothreitol, were prepared and stored in an anaerobic glove box (Coy Laboratory Products, Inc., Grass Lake, MI). Dithiothreitol was freshly prepared each day, as it is unstable in water. Within the anaerobic chamber, the reagents were added in the above quantities to a 4.5 mL optical glass cuvette (Starna Cells, Inc., Atascadero, CA) fitted with 10 mm screw caps

(SCHOTT Corp., Yonkers, NY) and 13 mm butyl rubber stoppers (Bellco Glass, Inc., Vineland, NJ). The cuvette was then removed from the chamber and purged with 100% H_2 for approximately 1 min using a 23G long stainless steel needle as the inlet and a short 22G needle as the outlet. The cuvette was placed in a 30°C receptacle of a spectrophotometer (Varian, Inc., Palo Alto, CA). A gas-tight syringe was used to transport approximately 0.5 mL of anoxic broth from the flask to the cuvette, after which the cuvette was shaken vigorously, placed in the spectrophotometer, and the absorbance (Abs) recorded at 546 nm every 0.5 s. Whole-cell broth was used for the enzyme assay since syngas fermentation is a whole-cell application. The quantified effects of NO in the whole-cell environment would be beneficial for developing a feasible gasification–fermentation system.

The concentration (C_{BV}) of reduced benzyl viologen (following the acceptance of electrons from H_2 consumption) was obtained from $C_{BV} = Abs/(\varepsilon \cdot b)$, where b is the cuvette path length (1 cm) and ε is the extinction coefficient for benzyl viologen (7.55 $mM^{-1}cm^{-1}$ at 546 nm). The maximum volumetric rate of benzyl viologen reduction (R_{BV}) was calculated from the linear slope of the initial portion of the curve following the short lag phase ($R_{BV} = \Delta C_{BV}/\Delta t$). Since 2 moles of benzyl viologen are reduced per mole of H_2 consumed, the volumetric rate of H_2 consumption (R_{H2}) was calculated as $1/2R_{BV}$. R_{H2} was finally divided by the measured cell density and converted into specific activity (U/mg) where one U represents one μmol of H_2 consumed per minute.

For the cell density, samples were collected in 4 mL cuvettes and the OD was measured at 660 nm using a UV-Vis spectrophotometer. The OD is proportional to the cell density ($\sim$ 0.43 g/L per OD unit) as obtained from a standard calibration chart showing a linear range of cell density between 0 and 0.4 OD units. Samples with an OD greater than 0.4 units were diluted so that the OD was within the linear range of calibration.

Product and Gas Analysis

Once the cell density and pH were measured, the samples from the flasks were centrifuged at 14,000 rpm for 10 min. The cell-free supernatant was then analyzed for ethanol and acetic acid using a 6890 Gas Chromatograph (Agilent Technologies, Wilmington, DE) with a flame ionization detector and an 8 ft Porapak QS 80/100 column (Alltech, Deerfield, IL).

Gas samples were taken periodically to measure the CO, CO_2, H_2, and NO concentrations in the inlet and outlet gas streams. Two 6890 Gas Chromatographs (Agilent Technologies), each with a TCD, were used to measure CO, CO_2, and H_2. A Chemiluminescence analyzer (Sievers) was used to measure the NO concentration. To convert NO and H_2 to aqueous concentrations, aqueous solubilities of 1.8 mM/atm for NO and 0.78 mM/atm for H_2 were used (Sander, 1999).

Results and Discussion

Cell Growth

Figure 2 shows the effect of 130 ppm (0.234 μM) NO on the growth of *C. carboxidivorans* P7[T]. Flask A (with no initial NO exposure) showed a typical growth profile with a lag phase, exponential phase, and stationary phase. The cell growth maximized at 0.24 OD and essentially remained stationary. On Day 4, 130 ppm NO was continuously added to flask A and the cell concentration increased to 0.35 OD towards the end of the experiment. In contrast, no cell growth was observed in Flask B when the cells were initially exposed to a continuous stream of 130 ppm NO. However, once the NO was removed on Day 4, the cells began to grow to a stationary OD of 0.24, similar to the stationary OD observed with Flask A in the absence of NO. These results demonstrate that the NO inhibition on initial cell growth is reversible.

In contrast to the 130 ppm experiment, no cell-growth inhibition occurred upon an initial exposure to 40 ppm (0.072 μM). Thus, the 40 ppm experiment and the experiment without initial NO exposure showed similar growth profiles. However, at 100 ppm NO (and higher), growth profiles mimicked the patterns observed with 130 ppm.
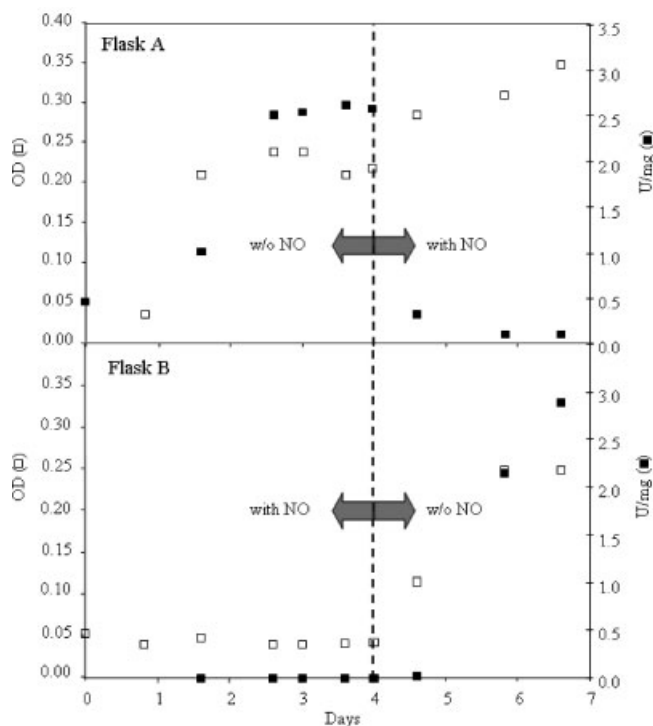
Hydrogenase Activity

As shown in Figure 2 for no initial NO exposure in Flask A, the specific activity of hydrogenase increased with time, reaching a maximum value of about 2.5 U/mg. Since the specific activity is per unit of cell mass, hydrogenase was upregulated during this time. Once 130 ppm NO was continuously introduced, the activity dropped to a steady value of approximately 0.1 U/mg. In Flask B where the cells were initially exposed to 130 ppm NO, the hydrogenase activity was negligible since the cells did not grow. Following the removal of NO, the specific hydrogenase activity increased with cell growth and reached a maximum of 2.8 U/mg, similar to the activity level observed in Flask A without any exposure to NO. Thus, initial exposure to NO did not affect the upregulation of hydrogenase if the NO was removed.

Experimental results at other concentrations of NO showed that the hydrogenase activity was extremely sensitive to NO. In all studies with varying NO concentrations, the hydrogenase activity profile was similar to Flask A (Fig. 2) prior to the addition of NO. Following 40 ppm NO exposure (0.072 μM), the hydrogenase activity did not decrease. However, at NO exposure levels above 80 ppm, the activity decreased to a steady level. At 160 ppm (0.288 μM), there was a complete loss of activity by NO. Ten to ninety-five percent activity inhibition occurred between 60 and 130 ppm NO. Figure 3 shows a plot of the percent hydrogenase inhibition versus the continuous NO concentration in the gas phase. The solid line passing through the data points represents a model discussed below.

Although the previous experiments in which NO was initially exposed to the cells showed that the upregulation of
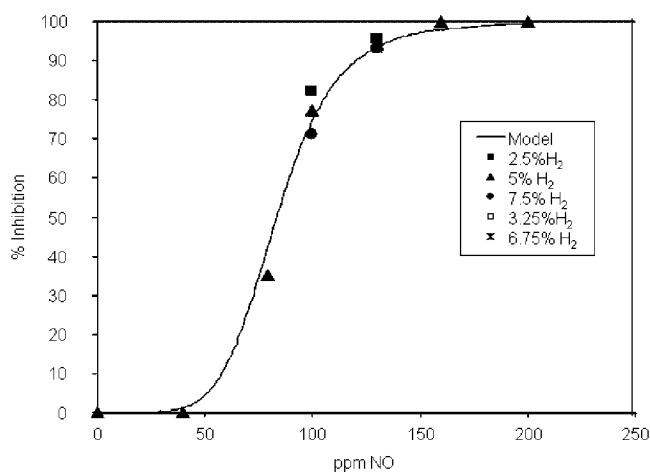

Figure 2. Optical density (OD) of cells at 660 nm and specific activity (U/mg) of hydrogenase. Flask A was exposed to a gas mixture without nitric oxide (NO) and Flask B was exposed to a gas mixture with NO. The dashed line represents the time at which the gases were switched so that Flask A now had NO in the gas stream while NO was absent in Flask B.

Figure 3. Percent inhibition of the hydrogenase enzyme with varying concentrations of nitric oxide and hydrogen. The solid line represents the model fit to Equation 1 in which % inhibition is the activity (*v*) in the presence of nitric oxide (NO) divided by the maximum activity in the absence of NO.

hydrogenase occurred after the NO was removed, the reversibility of activity loss needed to be assessed. In two experiments conducted with 200 ppm NO, the hydrogenase activity increased in the absence of NO and then was completely inhibited once the NO was added. However, the NO was again removed and it was observed that the hydrogenase activity returned to the previous level. Thus, the loss of hydrogenase activity is reversible.

Hydrogenase Kinetic Model

To assess the hydrogenase kinetic model in the presence of NO, Figure 4 shows the double reciprocal plot of $1/v$ versus $1/[H_2]$ where v is the hydrogenase activity (μmoles min^{-1} mg^{-1}). To appropriately compare the hydrogenase activity between experiments, the activities plotted in Figure 4 were obtained by dividing the activity by the maximum activity in the absence of NO (e.g., in Fig. 2, the maximum activity is shown at 4 d for Flask A) and then multiplying by the average of the maximum activities observed in all experiments. The plot is shown for NO concentrations of 0, 0.18 μM (100 ppm), and 0.234 μM (130 ppm) and aqueous H_2 concentrations varying from 18–110 μM (2.5–15% in the gas phase). As seen, the lines connecting data for each concentration of NO assessed converged on the negative x-axis, indicating that NO is a non-competitive inhibitor of the enzyme.

Equation 1, which was derived by combining a typical model for allosteric enzymes (Shuler and Kargi, 1992) with the non-competitive enzyme inhibition model (Roberts 1977), characterizes the hydrogenase activity in the presence of inhibition by NO:

$$v = \frac{V_m}{\left[1 + \frac{K_m}{[H_2]}\right]\left[1 + \left(\frac{[NO]}{K_{NO}}\right)^h\right]} \tag{1}$$

V_m represents the maximum hydrogenase activity (under the experimental conditions of this study), K_m is the Michaelis constant for H_2, K_{NO} is the inhibition constant for NO, and h is a constant for allosteric enzymes that generally refers to the number of interactive binding sites with the inhibitor. Equation 1 is the model shown in Figure 3 using the fitted parameters noted below.

The double-reciprocal plot for Equation 1 is:

$$\frac{1}{v} = \frac{K_m}{V_m}\left[1 + \left(\frac{[NO]}{K_{NO}}\right)^h\right]\frac{1}{[H_2]} + \frac{1}{V_m}\left[1 + \left(\frac{[NO]}{K_{NO}}\right)^h\right] \tag{2}$$

Regression analysis of the data in Figure 4, as applied to Equation 2, resulted in $K_m = 37.4 \pm 2.3$ μM, $V_m = 4.8 \pm 2.0$ U/mg, $h = 6.1 \pm 0.25$, and $K_{NO} = 0.141 \pm 0.001$ μM (95% confidence intervals). This indicates a possibility that NO could be interacting with up to six sites on the enzyme if NO binds as a first-order reaction (Hyman and Arp, 1988). NO can also interact with many species as a second-order reaction (Davis et al., 2001) and thus the interaction sites would be ½ of h or three sites. The possibility of multiple sites of inhibitor-binding has been addressed by Hyman and Arp (1991), who suggested that NO interacts with at least two distinct hydrogenase sites in *A. vinelandii*, possibly at the Fe-S centers. Further, it has also been seen that certain hydrogenases, like the Fe-only hydrogenase of *Clostridium pasteurianum*, have up to five distinct [Fe-S] clusters (Peters et al., 1998). Therefore, numerous binding sites for NO are feasible, although the details of hydrogenase binding domains for *C. carboxidivorans* P7[T] have not been assessed. The K_m value of 37.4 μM for H_2 is similar to the literature value of 37 μM (Schneider and Schlegel, 1976) for a purified enzyme study conducted on the hydrogenase of *A. eutrophus* H16 in the absence of any inhibitor (such as NO). This similarity suggests that the kinetics involving NO may also be similar to a purified enzyme study, although this has not been validated. However, understanding the kinetics in a whole-cell environment is important for quantifying the levels of NO that can be tolerated by cells in a gasification–fermentation system without compromising the hydrogenase activity.

Product Distribution

Figure 5 shows the product profile for the experiments shown in Figure 2. For Flask A, the acetic acid and ethanol concentrations reached approximately 0.96 g/L and 0.049 g/L, respectively, by Day 3.5 in the absence of NO. This is a typical trend seen in these cells as they produce more
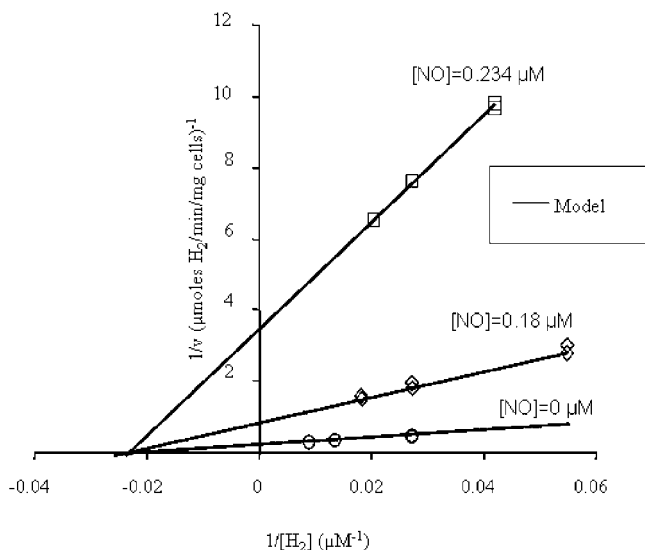

Figure 4. Double reciprocal plot showing the non-competitive inhibition of hydrogenase by nitric oxide (NO). The solid line represents Equation 2.
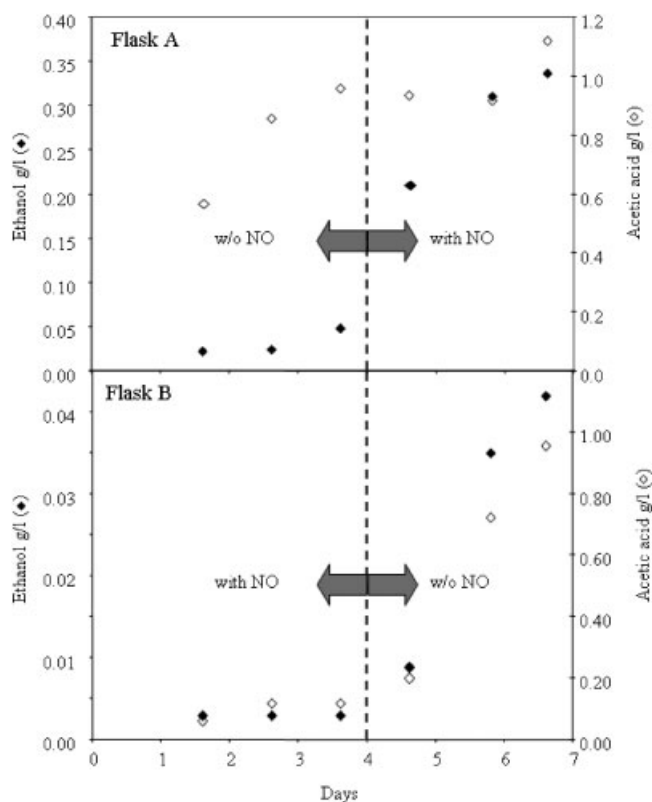
Figure 5. Ethanol and acetic acid profile. The experiment was the same as that shown in Figure 2. The dashed line represents the time at which the gases were switched so that Flask A now had NO in the gas stream while NO was absent in Flask B.

acid than ethanol during their growth phase. For Flask B, there was no significant growth when initially exposed to NO and the acetic acid and ethanol concentrations were 0.12 g/L and 0.003 g/L, respectively, by Day 3.5. Once Flask A was exposed to NO, the ethanol concentration started to increase drastically, reaching a value of about 0.337 g/L on Day 6.5. The acetic acid concentration stayed constant for approximately 2 days and then increased to a value of 1.12 g/L. This increase was perhaps linked to the increase in cell concentration in Flask A, as these cells tend to produce acetic acid during growth. When the NO exposure was removed from Flask B, the cells started growing and the acetic acid and ethanol concentrations increased to 0.96 g/L and 0.042 g/L, respectively. These concentrations are similar to the amounts produced in Flask A in the absence of NO. Thus, the introduction of NO in Flask A caused an increase in ethanol production and a slight increase in cell density.

The rapid rise in the ethanol concentration in Flask A following exposure to NO suggests that NO plays a role in the upregulation of ethanol production. Since the onset of solventogenesis is often associated with the onset of sporulation (Durre and Hollergschwandner, 2004), it is feasible that NO promotes solventogenesis and sporulation may eventually occur. The possible onset of sporulation was not assessed in this study. The drastic increase in ethanol concentration could not have been merely a pH effect as the pH of the culture medium in Flask A was at approximately 5.7 when the ethanol production increased following NO exposure. In contrast, the pH in Flask B (when the NO was removed) dropped from 6.0 to 5.7 but the ethanol produced by these cells was only 0.042 g/L. The fact that both flasks had similar ethanol concentrations in the absence of NO and Flask A showed a drastic increase in ethanol concentration on exposure to NO indicates that the product re-distribution is a result of NO and not the pH.

Interestingly, the increase in ethanol concentration was a result also seen in previous studies with biomass-syngas (Datar et al., 2004) indicating that NO may also be the cause of the product re-distribution seen in the presence of biomass-syngas. Thus, it appears that NO affects both the hydrogenase enzyme and the product re-distribution. As an extension of this work, recent studies showed that NO increases the activity of alcohol dehydrogenase, an enzyme responsible for the formation of ethanol (see Fig. 1), although the details of this work are beyond the scope of this article (Ahmed, 2006).

Conclusions

This work confirmed the hypothesis that NO measured in biomass-syngas was the cause of hydrogenase inhibition in *C. carboxidivorans* P7[T]. NO not only inhibited the hydrogenase, but also led to an increase in ethanol production by the cells. However, the loss of hydrogenase activity is reversible. Since other syngas-fermenting organisms utilize the same metabolic pathways, the potential of similar effects of NO on the fermentation process should be considered. Though it is desirable for cells to produce high amounts of ethanol, the presence of NO in biomass-syngas may not be entirely advantageous. As NO inhibits the hydrogenase activity, electrons for ethanol formation must come from CO rather than H_2, thus reducing the available carbon for product formation. This would reduce the carbon conversion efficiency of the process. Another problem that arises in the presence of NO is the initial growth inhibition. Removal of NO from the biomass-syngas may therefore alleviate these problems and allow the H_2 to supply the required electrons. The reduction in NO could be done either by increasing the efficiency of the gasification system to eliminate any combustion that may be occurring (NO is produced during combustion but not gasification) (West et al., 2005) or by scavenging NO using sodium hypochlorite, potassium permanganate, or sodium hydroxide (Brogren et al., 1997; Chu et al., 2001; Sada et al., 1978). However, this study shows that NO concentrations below 40 ppm have no effect on cell growth, hydrogenase activity, or product re-distribution for *C. carboxidivorans* P7[T]. Therefore, to minimize the effects of NO on any syngas-fermentation system, an initial estimate is to keep the NO concentration in biomass-syngas below 40 ppm.

References

Abrini J, Naveau H, Nyns EJ. 1994. Clostridium autoethanogenum, sp-nov, an anaerobic bacterium that produces ethanol from carbon monoxide. Arch Microbiol 161(4):345–351.

Acosta F, Real F, Ruiz de Galarreta CM, Diaz R, Padilla D, Ellis AE. 2003. Toxicity of nitric oxide and peroxynitrite to Photobacterium damselae subsp. Piscicida. Fish Shellfish Immunol 15(3):241–248.

Ahmed A. 2006. Effects of biomass-generated syngas on cell-growth, product distribution and enzyme activities of Clostridium carboxidivorans P7[T] [Ph.D. Dissertation]. Stillwater, OK: Oklahoma State University. 227 p.

Ahmed A, Cateni BG, Huhnke RL, Lewis RS. 2006. Effects of biomass-generated producer gas constituents on cell-growth, product-distribution and hydrogenase activity of Clostridium carboxidivorans P7[T]. Biomass Bioenerg 30(7):665–672.

Bridgwater AV. 1994. Catalysis in thermal biomass conversion. Appl Catal A: General 116(1–2):5–47.

Brogren C, Karlsson HT, Bjerle I. 1997. Absorption of NO in an alkaline solution of $KMnO_4$. Chem Eng Technol 20(6):396–402.

Chu H, Chien TW, Li SY. 2001. Simultaneous absorption of SO_2 and NO from flue gas with $KMnO_4$/NaOH solutions. Sci Total Environ 275(1–3):127–135.

Datar RP, Shenkman RM, Cateni BG, Huhnke RL, Lewis RS. 2004. Fermentation of biomass-generated producer gas to ethanol. Biotechnol Bioeng 86(5):587–594.

Davis K, Martin E, Turko IV, Murad F. 2001. Novel effects of nitric oxide. Annu Rev Pharmacol Toxicol 41:203–236.

Devi L, Ptasinski KJ, Janssen FJJG. 2003. A review of the primary measures for tar elimination in biomass gasification processes. Biomass Bioenerg 24(2):125–140.

Durre P, Hollergschwandner C. 2004. Initiation of endospore formation in Clostridium acetobutylicum. Anaerobe 10(2):69–74.

He B-Q, Wang J-X, Hao J-M, Yan X-G, Xiao J-H. 2003. A study on emission characteristics of an EFI engine with ethanol blended gasoline fuels. Atmos Environ 37(7):949–957.

Hsieh W-D, Chen R-H, Wu T-L, Lin T-H. 2002. Engine performance and pollutant emission of an SI engine using ethanol-gasoline blended fuels. Atmos Environ 36(3):403–410.

Hyman MR, Arp DJ. 1988. Reversible and irreversible effects of nitric oxide on the soluble hydrogenase from Alcaligenes eutrophus H16. Biochem J 254(2):469–475.

Hyman MR, Arp DJ. 1991. Kinetic analysis of the interaction of nitric oxide with the membrane-associated, nickel and iron-sulfur-containing hydrogenase from Azotobacter vinelandii. Biochim Biophys Acta 1076(2):165–172.

Kim BH, Bellows P, Datta R, Zeikus JG. 1984. Control of carbon and electron flow in Clostridium acetobutylicum fermentations—Utilization of carbon-monoxide to inhibit hydrogen-production and to enhance butanol yields. Appl Environ Microb 48(4):764–770.

Krasna AI, Rittenberg D. 1954. The inhibition of hydrogenase by nitric oxide. Proc Nat Acad Sci 40(4):225–227.

Liou JS-C, Balkwill DL, Drake GR, Tanner RS. 2005. Clostridium carboxidivorans sp. Nov., a solvent-producing clostridium isolated from an agricultural settling lagoon, and reclassification of the acetogen Clostridium scatologenes strain sl1 as Clostridium drakei sp. Nov. Int J Syst Evol Microbiol 55(5):2085–2091.

Nadim F, Zack P, Hoag GE, Liu S. 2001. United States experience with gasoline additives. Energ Policy 29(1):1–5.

Peters JW, Lanzilotta WN, Lemon BJ, Seefeldt LC. 1998. X-ray crystal structure of the fe-only hydrogenase (CPI) from Clostridium pasteurianum to 1.8 angstrom resolution. Science 282(5395):1853–1858.

Ragsdale SW. 1991. Enzymology of the acetyl-CoA pathway of CO_2 fixation. Critical Rev Biochem Mol Biol 26:261–300.

Roberts DV. 1977. Enzyme kinetics. Cambridge Eng, Vol. x. New York: Cambridge University Press. , 326 p.

Sada E, Kumazawa H, Kudo I, Kondo T. 1978. Absorption of NO in aqueous mixed solutions of $NaClO_2$ and NaOH. Chem Eng Sci 33(3):315–318.

Sander R. 1999. Compilation of Henry's law constants for inorganic and organic species of potential importance in environmental chemistry Mainz, Germany.

Schneider K, Schlegel HG. 1976. Purification and properties of soluble hydrogenase from Alcaligenes eutrophus H16. Biochim Biophys Acta 452(1):66–80.

Seefeldt LC, Arp DJ. 1989. Oxygen effects on the nickel-containing and iron-containing hydrogenase from Azotobacter vinelandii. Biochemistry 28(4):1588–1596.

Shenkman RM. 2003. C. Carboxidovorans culture advances and the effects of pH, temperature, and producer gas on key enzymes [M.S Thesis]. Stillwater: Oklahoma State University. 182 p.

Shuler ML, Kargi F. 1992. Bioprocess engineering: Basic concepts, Vol. xvi. Englewood Cliffs, NJ: Prentice Hall. 479 p.

Spath PL, Dayton DC. 2003. Preliminary screening—Technical and economic assessment of synthesis gas to fuels and chemicals with emphasis on the potential for biomass-derived syngas Golden, Colorado 80401–3393: National Renewable Energy Laboratory.

Tibelius KH, Knowles R. 1984. Hydrogenase activity in Azospirillum brasilense is inhibited by nitrite, nitric oxide, carbon monoxide and acetylene. J Bacteriol 160(1):103–106.

Vega JL, Clausen EC, Gaddy JL. 1990. Design of bioreactors for coal synthesis gas fermentations. Resour Conservation Recycl 3(2–3):149–160.

West DL, Montgomery FC, Armstrong TR. 2005. ''NO-selective'' NOx sensing elements for combustion exhausts. Sens Actuators B: Chemical. 111–112 84–90.

Yuksel F, Yuksel B. 2004. The use of ethanol-gasoline blend as a fuel in an SI engine. Renewable Energy 29(7):1181–1191.